ACS APPLIED MATERIALS & INTERFACES

Research Article

www.acsami.org

Injectable Dopamine-Modified Poly(ethylene glycol) Nanocomposite Hydrogel with Enhanced Adhesive Property and Bioactivity

Yuan Liu,[†,§] Hao Meng,[†,§] Shari Konst,[‡] Ryan Sarmiento,[†] Rupak Rajachar,[†] and Bruce P. Lee*[,†]

[†]Department of Biomedical Engineering and [‡]Department of Chemistry, Michigan Technological University, Houghton, Michigan 49931, United States

Supporting Information

ABSTRACT: A synthetic mimic of mussel adhesive protein, dopamine-modified four-armed poly(ethylene glycol) (PEG-D4), was combined with a synthetic nanosilicate, Laponite ($Na^{0.7+}(Mg_{5.5}Li_{0.3}Si_8)O_{20}(OH)_4)^{0.7-}$), to form an injectable naoncomposite tissue adhesive hydrogel. Incorporation of up to 2 wt % Laponite significantly reduced the cure time while enhancing the bulk mechanical and adhesive properties of the adhesive due to strong interfacial binding between dopamine and Laponite. The addition of Laponite did not alter the degradation rate and cytocompatibility of PEG-D4 adhesive. On the basis of subcutaneous implantation in rat, PEG-D4 nanocomposite hydrogels elicited minimal inflammatory response and exhibited an enhanced level of cellular infiltration as compared to Laponite-free samples. The addition of Laponite is potentially a simple and effective method for promoting bioactivity in a bioinert, synthetic PEG-based adhesive while simultaneously enhancing its mechanical and adhesive properties.

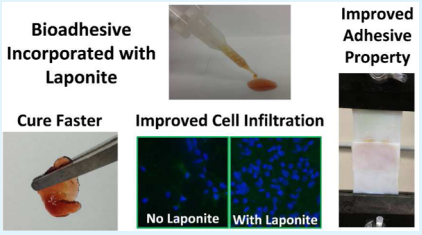

KEYWORDS: *mussel adhesive proteins, biomimetic tissue adhesive, dopamine, Laponite, cell infiltration, subcutaneous implantation*

INTRODUCTION

Tissue adhesives are widely used in surgery for wound closure, sealing suture lines, fixating of implants, and functioning as a hemostatic agent.[1−3] Tissue adhesives can simplify complex procedures, reduce surgery time, and minimize trauma. However, there are limitations associated with existing commercial adhesives. Fibrin glue (e.g., Tisseel, Baxter, Inc.) is hampered by weak adhesive properties and the risk for transferring blood-borne diseases (e.g., HIV, hepatitis).[4−6] Although cyanoacrylate-based adhesive (e.g., Dermabond, Ethicon, Inc.) exhibits excellent adhesive strength, it releases a toxic degradation product (formaldehyde), has poor biomechanical compatibility with the repaired tissues, and degrades over an extremely long period of time (>3 years).[7,8] Synthetic adhesives consisting of biocompatible polyethylene glycol (PEG; e.g., CoSeal, Baxter, Inc.) have poor mechanical properties and may swell excessively to apply pressure to surrounding tissues (e.g., nerve compression).[9,10] Additionally, PEG-based hydrogels act as a barrier to tissue ingrowth and wound healing.[11] Thus, there is a continued need for the development of biocompatible and biodegradable tissue adhesives with superior adhesive strengths.

Marine mussels secrete adhesive proteins that enable these organisms to attach to surfaces (rocks, boats, etc.) in a wet, saline environment.[12,13] These proteins contain as much as 28 mol % of a catecholic amino acid, 3,4-dihydroxyphenylalanine (DOPA), which plays an important role in interfacial binding and intermolecular cross-linking.[14] The catechol is a unique and versatile adhesive molecule capable of binding to both inorganic and organic surfaces through either reversible or covalent bonds. Catechol forms strong, reversible bonds with metal oxides with bond strength reaching 40% that of a covalent bond.[15] This is the strongest reversible bond involving a biological molecule reported to date. When catechol is oxidized to form the highly reactive quinone, it participates in intermolecular covalent cross-linking, leading to the rapid curing of catechol-containing adhesives,[16,17] and reacts with nucleophile (i.e., $-NH_2$, $-SH$) found on biological substrates, resulting in strong interfacial binding.[15,18] Catechol-modified bioadhesvie materials demonstrated potential in sutureless wound repair,[19] sealing of fetal membranes,[20,21] Achilles tendon repair,[22] cell engineering,[23,24] and local delivery of therapeutic drug particles.[25]

In this study, we combined a biomimetic PEG-based adhesive with a synthetic, biodegradable nanosilicate, Laponite ($Na^{0.7+}(Mg_{5.5}Li_{0.3}Si_8)O_{20}(OH)_4)^{0.7-}$), to create a novel nanocomposite tissue adhesive. Laponite has similar chemical composition as bioactive glass and mimics some of its biological properties.[26−28] Laponite degrades into nontoxic products (Na^+, $Si(OH)_4$, Mg^{2+}, Li^+) at neutral pH.[29] Orthosilicic acid ($Si(OH)_4$) is naturally found in numerous human tissues and organs (e.g., bone, tendon, liver, and kidney tissues),[30] and it had been demonstrated to promote synthesis of type I collagen and osteoblast differentiation in human osteosarcoma cells in vitro.[31] Mg^{2+} ions also play an important role in mediating cellular adhesion.[32] Incorporation of Laponite into bioinert polymeric networks promoted cell attachment and proliferation while greatly enhanceing the mechanical properties of these

Received: July 14, 2014
Accepted: September 15, 2014
Published: September 15, 2014

materials.[33,34] Recently, our lab demonstrated that the strong interfacial binding between Laponite and network-bound dopamine greatly enhanced the mechanical strength and toughness of nanocomposite hydrogels.[35]

Here, we combined Laponite with an injectable PEG-based adhesive that is modified with biomimetic catechol adhesive moiety (PEG-D4, Scheme 1). The effect of Laponite incorporation on the curing rate, degradation rate, mechanical and adhesive properties, and biocompatibility (both in culture and in a rat subcutaneous model) of the nanocomposite bioadheisve were evaluated.

Scheme 1. Chemical Structure of PEG-D4

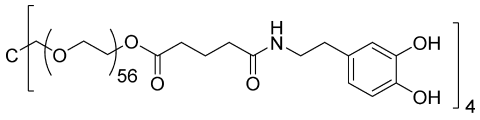

EXPERIMENTAL SECTION

Materials. Sodium periodate ($NaIO_4$, >99.8%) was obtained from Acros Organics (Fair Lawn, NJ). Bovine pericardium was purchased from Sierra for Medical Science (Whittier, California). 3-(4,5-dimethylthiazol-2-yl)-2,5-diphenyltetrazolium bromide 98% (MTT) was from Alfa Aesar (Ward Hill, MA). 1X phosphate buffer saline was from Fisher Scientific Co. (Pittsburgh, PA). Histology mounting medium polyfreeze, Trichrome Stain (Masson) Kit, bouin solution, and Weiger's iron hematoxylin solution were purchased from Sigma-Aldrich (St. Louis, MO). Anti-S100A4 antibody (ab27957), goat antirabbit IgG H&L (Alexa Fluor 488) (ab150077), anti-CD68 antibody (ab125212), and goat antirabbit IgG H&L (Alexa Fluor 647) were purchased from Abcam (Cambridge, MA). 4′,6-Diamidino-2-phenylindole (DAPI) was obtained from Invitrogen (Grand Island, NY). Laponite XLG (Laponite) was a gift from Southern Clay Products, Inc. (Austin, TX). PEG-D4 was prepared as previously described.[36]

Preparation of PEG-D4 Nanocomposite Hydrogels and Curing Time Testing. Hydrogels were formed by mixing equal volumes of the polymer precursor solution (300 mg/mL PEG-D4 in 20 mM phosphate buffer solution at pH 7.4) and $NaIO_4$ solution (54.5 mM in deionized H_2O with 0−4 wt % Laponite). The concentrations of the respective constituents in the hydrogel are diluted by half after mixing, so that the concentrations of PEG-D4 and Laponite were kept at 150 mg/mL and 0−2 wt %, respectively. The final $NaIO_4$-to-dopamine molar ratio ranged from 0.1 to 1.5. The time it took for the adhesive to cure was determined when the mixture ceased to flow in a tilted vial.[37] Unless specified otherwise, all hydrogels were allowed to cure for 24 h and equilibrated in phosphate-buffered saline (PBS) (pH = 7.4) for further characterizations.

Characterization of PEG-D4 Nanocomposite Hydrogels. Hydrogels were equilibrated in PBS (pH = 7.4) overnight and then vacuum-dried for at least 2 d to obtain dry gels. Fourier transform infrared (FTIR) spectra of the dried samples were obtained using a PerkinElmer Spectrum One spectrometer. Equilibrium water content (EWC) was defined as

$$\mathrm{EWC} = \frac{M_s - M_d}{M_s} \times 100\% \quad (1)$$

where M_s and M_d denote the mass of swollen and dry hydrogels, respectively.

In Vitro Degradation. Hydrogel discs (diameter = 10 mm, thickness = 1.5 mm, n = 3) were transferred into vials containing 5 mL of PBS (pH = 7.4) and incubated at 37 °C. The PBS solution was removed and replaced with fresh PBS every 7 d. At a specific time, samples were dried to determine their remaining mass (M_t) at time t. The percent residual mass of hydrogels was determined by

$$\text{residual dry mass\%} = \frac{M_t}{M_0} \times 100\% \quad (2)$$

where M_0 is the average dry mass of three samples that did not undergo degradation.

Compression Testing. Unconfined, uniaxial compression testing was performed using a servohydraulic materials testing system (8872 Instron, Norwood, MA). Hydrogels (number of repeat n = 3) were compressed at a rate of 1.8 mm/min until the sample fractured. The dimensions of each hydrogel (diameter ≈ 10 mm; thickness ≈ 5 mm) were measured using a digital caliper immediately before testing. Stress was determined based on the measured load divided by the initial surface area of the sample. Strain was determined by dividing the change in the position of the compressing plate by the initial thickness of the hydrogel. Toughness was determined by the integral of the stress−strain curve. The elastic modulus was taken from the slope of the stress−strain curve between a strain of 0.05 and 0.2.

Oscillatory Rheometry. Rheological properties of the nanocomposite hydrogels were characterized using a Bohlin C-VOR 200 NF rheometer. Frequency sweeps (0.01−100 Hz at 0.1 strain) were performed to determine the storage (G') and loss (G'') moduli. Hydrogel discs (diameter = 25 mm, thickness = 1.5 mm, n = 3) were tested using parallel plates at a gap distance that is set at 87.5% of the individual hydrogel thickness, as measured by a digital caliber. Mineral oil was applied around the edge of the hydrogel to prevent dehydration.

Lap Shear Adhesion Testing. Adhesive properties of hydrogels were determined by using lap shear adhesion test according to American Society for Testing and Materials (ASTM) standard F2255−05.[38] Bovine pericardium were cut into 2.5 cm × 2.5 cm strips and hydrated in PBS. PEG-D4 nanocomposite hydrogels were cured between two partially overlapping bovine pericardium with an overlapping area of 2.5 cm × 1 cm. The adhesive joint was compressed with a 100 g weight for 10 min and further conditioned in PBS (pH = 7.4) at 37 °C for overnight prior to testing. A commercial PEG-based sealant, CoSeal (Baxter, Inc.), was prepared the same way and tested for comparison. The dimensions of contact area of each adhesive joint were measured using a digital caliper immediately before testing. The adhesive joints were pulled to failure at a rate of 5 mm/min until the tissues separated, using a servohydraulic materials testing system (8872 Instron, Norwood, MA). The adhesive strength and work of adhesion were determined by the max load and integral area of load versus displacement curve divided by the initial contact area of the adhesive joint, respectively.[39]

Cell Culture and in Vitro Cytotoxicity Study. Cytotoxicity was evaluated by determining the viability of cells exposed to the hydrogel extracts,[19,40] as measured using quantitative MTT assay according to ISO 10993−5 guideline.[41] L929 mouse fibroblasts were cultured in Dulbecco's modified Eagle's medium (DMEM) containing 10% fetal bovine serum (FBS) and 10 units/ml penicillin−streptomycin at 37 °C in 5% CO_2 humidified atmosphere. Hydrogels were cut into disc shape (5 mm diameter, 2 mm thick) and sterilized using two methods (ethanol[42] and sterile filtration[19]). For ethanol-based sterilization, hydrogels were submerged in 70% (v/v) ethanol for 45 min followed by washing three times with 20 mL of sterile PBS for 90 min. The hydrogels were then incubated in DMEM (10 mg/mL) for 24 h at 37 °C to obtain hydrogel extract. To test if ethanol sterilization method may potentially remove cytotoxic leachable materials, disc-shaped hydrogels were formed using unsterile precursor solutions and incubated in DMEM (10 mg/mL) for 24 h at 37 °C. The hydrogel extracts were then filtered through a 0.22 μm sterile filter to remove biological contamination factors. L929 cells were suspended in DMEM and seeded into 96-well microculture plates at a density of 10^4 cells/100 μL/well and incubated in humidified incubator (37 °C, 5% CO_2) for 24 h to obtain a confluent monolayer of cells; then the medium was replaced by 100 μL/well of hydrogel extract. The cells cultured in DMEM were set as control. After incubation for 24 h the medium was removed and replaced with 50 μL of MTT solution (1 mg/mL in PBS) and incubated for another 2 h. Finally all solution was removed, and 100 μL/well DMSO was added to dissolve the crystals completely.

Scheme 2. Schematic Representation of Applying the Nanocomposite Adhesive to Tissue by Mixing PEG-D4 with $NaIO_4$ and Laponite[a]

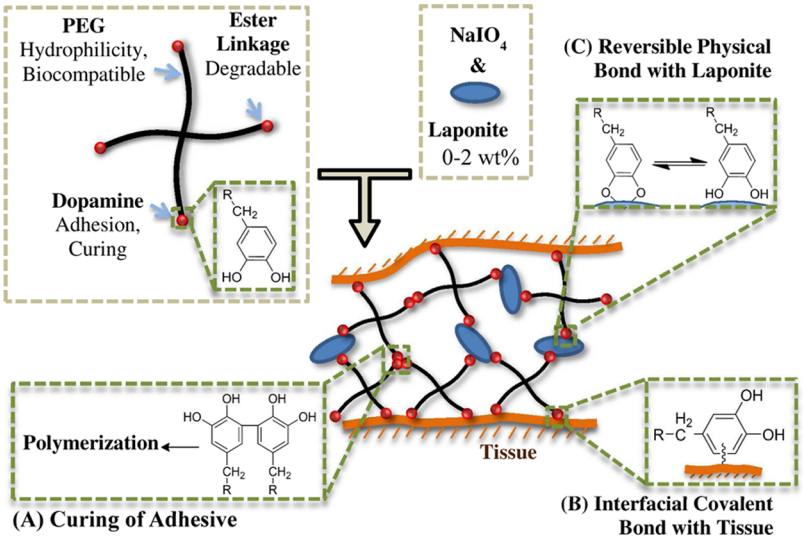

[a]Dopamine is capable of forming three types of crosslinks in this system: (A) covalent crosslinking and polymerization between dopamine moieties, resulting in curing of the adhesive, (B) interfacial covalent crosslinking between dopamine and functional groups (e.g., $-NH_2$) found on tissue surface, and (C) reversible physical crosslinks between dopamine and Laponite.

The absorbance of each well was measured at 570 nm (reference 650 nm) using a Synergy HT Multi-Mode Microplate Reader (BioTek, USA). The relative cell viability (mean% ± SD, $n = 3$) was expressed as

$$\text{cell viability\%} = \frac{\text{Abs}_{\text{hydrogel}}}{\text{Abs}_{\text{control}}} \times 100\% \quad (3)$$

where $\text{Abs}_{\text{hydrogel}}$ and $\text{Abs}_{\text{control}}$ are the absorbance for cells cultured in hydrogel extract and DMEM, respectively. For each hydrogel formulation (PEG-D4 with 0, 1, and 2 wt % Laponite), three independent cultures were prepared. Samples with relative cell viability less than 70% were considered to be cytotoxic.[43]

Subcutaneous Implantation. Healthy, weight-matched Sprague–Dawley rats were obtained from Michigan Technological University animal facility. PEG-D4 hydrogel and PEG-D4 nanocomposite hydrogel with 2 wt % Laponite discs (diameter = 10 mm, thickness = 1.5 mm) were bilaterally implanted subcutaneously in the backs of the Sprague–Dawley rats. The subcutaneous implantations were performed following the approved protocol by the Michigan Technological University Animal Committee (IACUC). Hydrogel samples were sterilized using the same procedure (ethanol-based sterilization) as in the in vitro cytotoxicity study.[42] Rats were anesthetized using an isofluorane–oxygen gas mixture, and fur around the implantation site was removed. A pouch was formed using a pair of fine scissors, and a hydrogel was placed in this pouch. Four and eight weeks postsurgery, the animals were sacrificed, and the implanted hydrogel along with surrounding skin tissues were collected, embedded in polyfreeze, and then flash frozen in liquid nitrogen. The frozen samples were stored in −80 °C freezer before sectioning. All tissues were cryosectioned into 10 μm thick sections and stained with Masson's trichrome staining for morphology and collagen production evaluation. Additionally, immunohistochemistry analysis was performed by staining the tissue sections with inflammatory cell marker CD68, fibroblast cell marker S100A4 for evaluating inflammatory cells invasion and fibroblasts infiltration. DAPI was used to locate the cells via staining the nuclei of cells. All histological imaging analyses were performed on an Olympus microscope. Trichrome staining was used to separate cellular rich layers (red color) close to implant interface from collagen layer (blue color).[44] Fluorescent staining was used to identify the main cell types (e.g., fibroblasts and macrophages) found at the implant interface. Cell infiltration and local collagen content were quantified by ImageJ.

Statistical Analysis. Statistical analysis was performed using Origin software. One-way analysis of variance (ANOVA) with Tukey HSD analysis and student t test were performed for comparing means of multiple groups and two groups, respectively, using a p-value of 0.05.

RESULTS AND DISCUSSION

Preparation of PEG-D4 Nanocomposite Hydrogels. A novel injectable nanocomposite adhesive was prepared by combining PEG-D4 and Laponite (Scheme 2). PEG, a hydrophilic, biocompatible polymer used in numerous Food and Drug Administration (FDA) approved products,[45] was employed as the major structural component for this tissue adhesive hydrogel. The four-armed PEG (10 kDa) was end-modified with glutaric acid and dopamine. PEG and glutaric acid are linked by a hydrolyzable ester linkage, and breaking of this bond results in adhesive degradation. Dopamine contains a catechol group that can be oxidized by oxidants (e.g., $NaIO_4$) to form highly reactive quinone that is capable of intermolecular cross-linking (Scheme 2A).[37,46] Additionally, quinone reacts with functional groups (i.e., $-NH_2$, $-SH$) found on biological tissue surfaces resulting in strong interfacial binding (Scheme 2B).[15,18] Finally, catechol forms strong physical interfacial bonds with Laponite, which greatly enhances the materials properties of the nanocomposite hydrogel (Scheme 2C).[35] Although samples characterized in this report were formed by simple mixing of the precursor solutions using pipet tips, the precursor solutions can be delivered and mixed using a dual-barreled syringe (Supporting Information, Figure S1).

The curing time of PEG-D4 hydrogels was strongly dependent on $NaIO_4$/dopamine molar ratios (Figure 1). Regardless of Laponite content, the fastest curing time was observed at a $NaIO_4$/dopamine molar ratio of 0.5. A similar trend has been previously reported for DOPA- and dopamine-modified PEG.[37,40] In periodate-mediated cross-linking, the reduced form of catechol cross-links with one of the oxidation

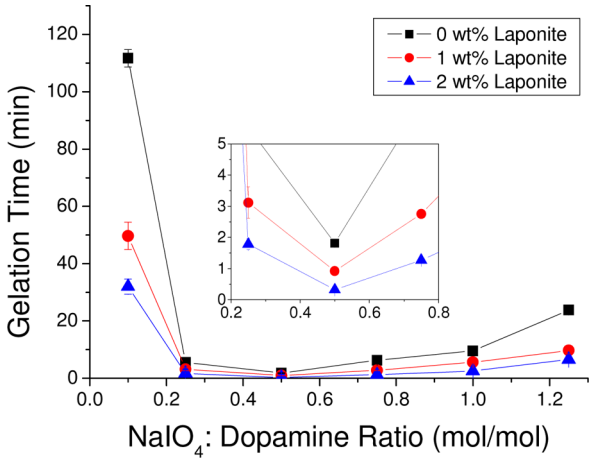

Figure 1. Curing time of PEG-D4 hydrogel as a function of $NaIO_4$/dopamine molar ratio with different Laponite concentrations. (inset) Graph of the results for $NaIO_4$/dopamine molar ratio between 0.2 and 0.8.

intermediates of catechol, α,β-dehydrodopamine.[47] As such, a nearly equal molar concentration of dopamine and $NaIO_4$ was needed to achieve fast curing. Additionally, incorporation of Laponite shortened the curing time for all the stoichiometric ratios of $NaIO_4$ and dopamine tested. For example, at a $NaIO_4$/dopamine molar ratio of 0.5, the curing times were 1.81 ± 0.12 min, 0.92 ± 0.03 min, and 0.33 ± 0.06 min for samples containing 0, 1, and 2 wt % Laponite, respectively. Strong interfacial binding between dopamine and Laponite resulted in the formation of physical cross-links within the nanocomposite network, which reduced the number of chemical cross-links needed for network formation and resulting in reduced cure time. Given a $NaIO_4$/dopamine molar ratio of 0.5 exhibited the optimal curing rate, subsequent tests were performed using samples prepared at this ratio.

Characterization of Nanocomposite Hydrogel. FTIR spectra confirmed the incorporation of Laponite into PEG-D4 network (Figure 2). The spectrum of PEG-D4 showed characteristic peaks for ether bonds (1000−1150 cm^{-1}, −C−O−C−), alkyl groups (2880 cm^{-1}, $-CH_2-$), and carbonyl (1729 cm^{-1}, ester bonds)[48] but no Si−O−Si peak (995 cm^{-1}) corresponding to that of Laponite.[49] The Si−O−Si peak was

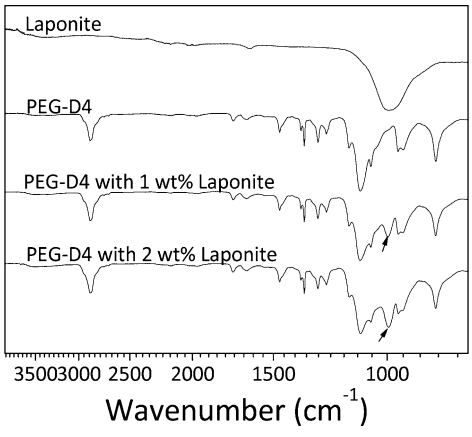

Figure 2. FTIR spectra of Laponite, PEG-D4, and PEG-D4 with 1 and 2 wt % Laponite. The arrows indicate the Si−O−Si peak in the nanocomposite hydrogel.

present in the nanocomposite networks (black arrows in Figure 2), which also increased in intensity with increasing Laponite concentration.

Equilibrium water content (EWC) averaged around 93 wt % for PEG-D4 hydrogels (Figure 3). Incorporating Laponite into

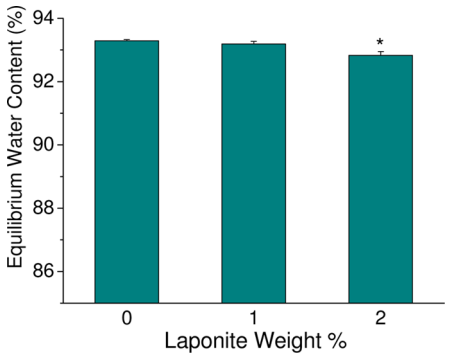

Figure 3. Equilibrium water content of PEG-D4 hydrogels cured using a $NaIO_4$/dopamine molar ratio of 0.5 and Laponite content of 0−2 wt %. * $p < 0.05$ when compared to 0 wt % Laponite.

PEG-D4 demonstrated marginal decrease in EWC value (93.3% ± 0.04% and 92.8 ± 0.12 for 0 and 2 wt % Laponite, respectively). EWC is a measure of the physical properties of a hydrogel network, and EWC values are inversely proportional to both the cross-linking density and the mechanical properties of a hydrogel.[50,51] These results indicated that a relatively small amount of Laponite used in our study did not significantly alter the cross-linking density of the PEG-D4 network.

Mechanical Testing of Nanocomposite Hydrogels. From unconfined compression testing, hydrogels containing Laponite exhibited a significant increase in both the maximum compressive stress, fracture strain, and toughness when compared to Laponite-free samples (Figure 4). The observed increase in these materials properties was presumably due to the increasing interfacial binding between Laponite and dopamine in the hydrogel. In the presence of external loads, breaking of dopamine-Laponite bonds occurs first while minimizing damage to the chemical cross-linked network, which means higher strength and energy were needed to fracture the more compliant nanocomposite than the Laponite-free hydrogels. Physical interactions between polymer matrix and the embedded nanoparticles have been previously reported to improve the fracture strength of hydrogels via reversible attach-detach processes.[52] However, there was no change in the elastic modulus. This observation is in agreement with results obtained from EWC analysis, which indicated that the incorporation of 1−2 wt % of Laponite did not drastically change the hydrogel cross-linking density.

The viscoelastic properties of the hydrogel were determined using oscillatory rheometry (Figure 5). For all the formulations tested, the storage modulus (G') values were greater than the loss moduli (G''), indicating the hydrogels were chemically cross-linked. For Laponite-containing samples, G' increased with increasing frequency, while G'' reached a plateau at 1 Hz. Similar observations have been reported for hydrogel cross-linked with both covalent and physical bonds.[53] Both measured G' and G'' values for hydrogel containing Laponite were significantly higher than those of Laponite-free samples (~1.5-fold and ~3-fold increases, respectively, at 1 Hz). An increase in the stiffness of hydrogels implies that the incorporation of

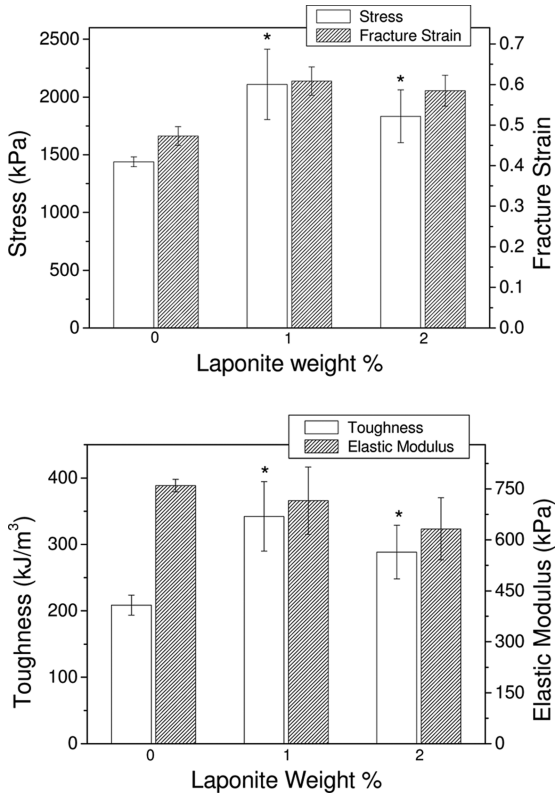

Figure 4. Results from compression testing of PEG-D4 hydrogels cured using a $NaIO_4$/dopamine molar ratio of 0.5 and Laponite content of 0−2 wt %. * $p < 0.05$ when compared to 0 wt % Laponite.

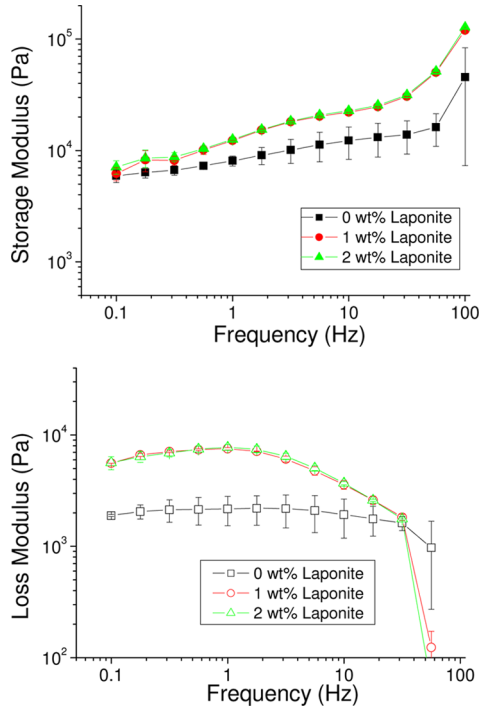

Figure 5. Storage and loss modulus of PEG-D4 hydrogels with $NaIO_4$/dopamine molar ratio of 0.5 containing up to 2 wt % Laponite subjected to oscillatory strain = 0.1 at a frequency of 0.1−100 Hz.

Laponite increased the cross-linking density of nanocomposite hydrogel. An increased G'' indicated that these nanocomposites demonstrated elevated viscous dissipation properties due to the presence of reversible bonds in the hydrogel network.[52−54] However, the increase in the measured G' values was marginal when compared to Laponite-free network, suggesting that there may not have been a drastic change in the network structure. There was also no difference between the rheological data for samples containing different amounts of Laponite.

From the measured G', hydrogel with Laponite showed less than 1.5-fold increase when compared to that of Laponite-free hydrogel. Similarly, EWC data and elastic modulus found from compression testing did not show much difference in values between these formulations. Taken together, we speculate that the cross-linking density of nanocomposite hydrogel was not significantly altered by the addition of 1−2 wt % of Laponite. These observations are potentially due to the location of dopamine as a terminal group in the four-armed-PEG polymer (Supporting Information, Scheme S1). For PEG-D4 samples with and without Laponite, formation of cross-links (e.g., dopamine polymerization and dopamine-Laponite) occurs at the terminal dopamine group. Therefore, little change in the molecular weight between cross-links occurred with the introduction of Laponite, even if there was strong interactions between Laponite and dopamine. Previously, we demonstrated that when dopamine is present as a side chain of a polymer network, a small addition of Laponite (1−3 wt %) formed new cross-linking points and resulted in an increase in the storage modulus by more than an order of magnitude and a large reduction in equilibrium water content (16−21% decrease).[35] Additionally, there is competitive cross-linking for dopamine (i.e., covalent cross-linking between dopamine and noncovalent dopamine-Laponite interaction), which may have also limited the number of dopamine for interacting with Laponite. These observations also suggest that the interaction between PEG chain and Laponite was relatively weak in our sample, and this interaction did not sufficiently alter the network architecture. Given that there was a statistical increase in measured toughness and loss moduli in the Laponite-containing networks, strong interfacial physical interaction mainly occurred between terminal dopamine moieties and Laponite, as illustrated in Scheme 2.

Lap Shear Adhesion Testing. Incorporation of Laponite significantly enhanced the adhesive properties of the nanocomposite hydrogels (Figure 6). PEG-D4 containing 2 wt % Laponite exhibited lap shear adhesive strength and work of adhesion values (7.9 ± 1.8 kPa and 16.8 ± 3.5 J/m^2, respectively) that were nearly 2.5-fold higher than those for Laponite-free PEG-D4 (3.5 ± 1.2 kPa and 6.7 ± 2.0 J/m^2, respectively). Observed increase in improved adhesive properties is attributed to the strong catechol−Laponite interaction, which required elevated fracture energy to separate the adhesive joint. When compared to mechanical testing results, incorporation of Laponite significantly increased the compressive properties and shear moduli of PEG-D4 hydrogels, indicating that increased bulk materials properties contributed to improved adhesive performance. These increases in the bulk materials properties allow the nanocomposite hydrogel to withstand more forces during the lap shear adhesion testing. This observation is consistent with previously published reports where bulk cohesive properties of an adhesive contribute to its adhesive properties.[55,56] In this work, PEG-D4 adhesive containing up to 2 wt % of Laponite achieved a good balance among the three competitive reactions that dopamine is capable of undergoing (Scheme 2), resulting in enhanced adhesive properties. PEG-D4 with and without Laponite also signifi-

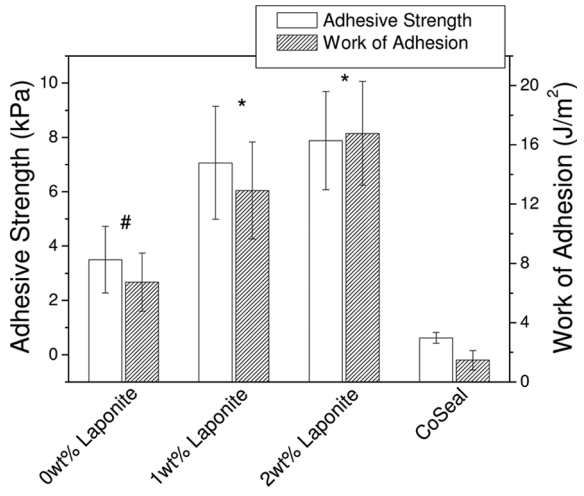

Figure 6. Lap shear adhesion test results of PEG-D4 hydrogels with $NaIO_4$/dopamine molar ratio of 0.5 containing up to 2 wt % Laponite. * $p < 0.05$ when compared to 0 wt % Laponite and CoSeal. # $p < 0.05$ when compared to CoSeal.

cantly outperformed CoSeal (Baxter, Inc., 0.6 ± 0.2 kPa and 1.5 ± 0.7 J/m^2, respectively), a commercially available PEG-based adhesive. The lap shear strength values reported here are lower when compared to previously published results for catechol-modified PEG systems with similar architectures, which range ~10−40 kPa.[57,58] However, it is not possible to compare these values directly due to differences in testing protocols (e.g., preparation of adhesive joint, strain rate, etc.) and substrates used.

In Vitro Degradation. The effect of Laponite content of the degradation rate of the PEG-D4 was determined by tracking the change in the dry mass of the samples over time (Figure 7). PEG-D4 lost over 70% of its dry mass over eight

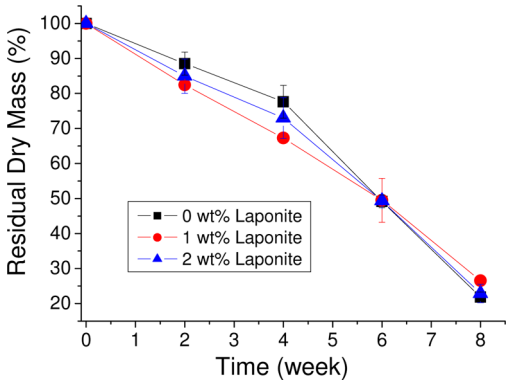

Figure 7. In vitro degradation of PEG-D4 hydrogels in PBS (pH = 7.4) at 37 °C. The values were normalized to the average dry mass of the hydrogels that did not undergo degradation.

weeks and completely degraded soon after. Incorporation of Laponite did not affect the degradation rate of the hydrogels, indicating that mass loss was driven by the hydrolysis of ester bond between PEG and glutaric acid. FTIR analysis of hydrogel containing 2 wt % of Laponite still shows a Si−O−Si peak with reduced intensity after eight weeks of degradation (Supporting Information, Figure S2), indicating that Laponite is still present in the hydrogel network.

MTT Assay. A quantitative MTT assay was used to determine the cytocompatibility of PEG-D4 nanocomposites (Figure 8). Regardless of sterilization methods and hydrogel

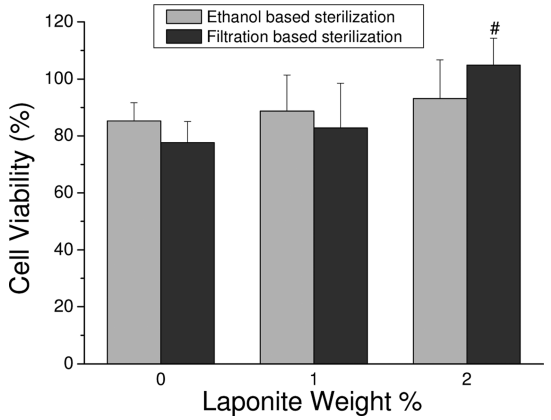

Figure 8. Relative cell viability of PEG-D4 hydrogels with up to 2 wt % Laponite. (left) Ethanol-based sterilization. (right) Filtration-based sterilization. # $p < 0.05$ when compared to 0 wt % Laponite normalized to medium control.

formulations, hydrogel extracts were found to be noncytotoxic, with relative cell viability greater than 75%. Other catechol-modified polymeric adhesives have been demonstrated to be noncytotoxic.[19,40,57] As expected, Laponite did not adversely affect the biocompatibility of PEG-D4 formulations as it was previously determined to be biocompatible with various cell types when incorporated into hydrogel.[34,59] Interestingly, relative cell viability for hydrogel containing 2 wt % Laponite was significantly higher than that of Laponite-free PEG-D4 hydrogel when the hydrogel extracts were sterile-filtered. Leachable ions from the degrading Laponite possibly had a proliferative effect on fibroblast. Using the ethanol sterilization method, these degradation products were likely removed during soaking in ethanol and repeated washings by PBS, and there were no significant differences in cell viability between formulations.

Subcutaneous Implantation. To further evaluate the biocompatibility of these materials, PEG-D4 with either 0 or 2 wt % Laponite was implanted subcutaneously in rat for four and eight weeks. After four weeks of implantation, the histological analysis results revealed the formation of fibrous capsule at the interface between the implant and the subcutaneous tissue as well as a cellular infiltration layer that is rich in fibroblasts (Figure 9). These observations resembled findings reported by others for degradable implants that promoted cellular infiltration.[44,60,61] Thicker fibrous capsules were observed for Laponite-containing hydrogels (Table 1), which may be associated with elevated proliferation and activation of fibroblasts, which up-regulated collagen production in the tissues surrounding the hydrogel.[44] Our hydrogel cytotoxicity testing results seem to indicate that leachable ions from Laponite support fibroblast proliferation (Figure 8). Although there was no difference in the thickness of infiltration layer between samples, there is a significantly higher cellular density for Laponite-containing hydrogels. The infiltration layers of 2 wt % Laponite hydrogels also consisted of a small amount of macrophage, while those of 0 wt % Laponite hydrogels were macrophage-free (Supporting Information, Figure S3). The release of inorganic ions from Laponite potentially contributed

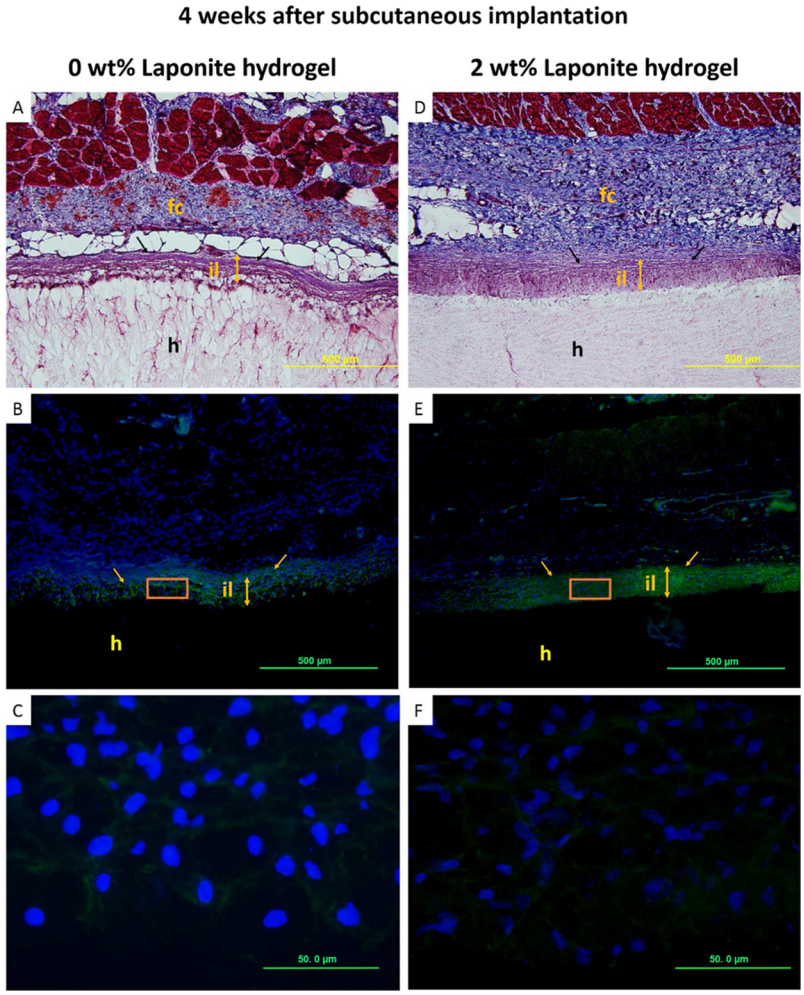

Figure 9. Histological characterization of PEG-D4 hydrogels containing 0 and 2 wt % Laponite and surrounding tissues after four weeks of subcutaneous implantation. Masson's trichrome staining images for evaluating the overall tissue section morphology and the thickness of the fibrous capsule (fc) (A, D). Immunohistochemical staining images for evaluating the infiltration cell type and density (B, C, E, F). Cell nuclei were stained by DAPI (blue), fibroblasts were stained by marker S100A4 (green). (C) and (F) are the enlarged view of the orange boxes in (B) and (E), respectively. "h": hydrogel; "il": infiltration layer; one-sided arrows: interface between hydrogel and tissue; two-sided arrows: the thickness of the infiltration layer.

Table 1. Fibrous Capsule Thickness, Inflammation Response, Cell Infiltration, and Infiltrated Cell Density Assessment of the Implanted PEG-D4 Hydrogels (0 and 2 wt % Laponite) and Surrounding Tissue Retrieved after Four and Eight Weeks of Subcutaneous Implantation

	four weeks		eight weeks	
	0 wt % Laponite	2 wt % Laponite	0 wt % Laponite	2 wt % Laponite
fibrous capsule thickness (μm)	253 ± 18.7	305 ± 41.2	498 ± 60.6	337 ± 77.9
	$p = 0.045^a$		$p = 0.0002^a$	
cell infiltration thickness (μm)	125 ± 15.1	126 ± 4.90	cells infiltrated throughout these samples	
	$p = 0.85^a$			
inflammatory response[b]	−	+	−	−
cell density (cells/mm^2)[c]	2530 ± 496	4510 ± 711	6860 ± 838	9580 ± 839
	$p = 0.020^a$		$p = 0.014^a$	

[a] $p < 0.05$ indicates significant difference (analyzed by t test). [b] "+" and "−" denote positive outcome and negative outcome, respectively. [c] Cell density within the infiltration layer and throughout the bulk of the hydrogels for week four and eight samples, respectively.

to the increased inflammatory response of the nanocomposite. Both trichrome and immunofluorescent staining indicated that no cells were observed inside the hydrogels.

After eight weeks, the thickness of fibrous capsule surrounding Laponite-free hydrogels nearly doubled, while the fibrous capsule thickness for hydrogels containing 2 wt % Laponite remained the same (Figure 10, Table 1). Qualitatively, Laponite-containing samples appeared smaller when explanted when compared to Laponite-free samples by week eight. The presence of macrophages and higher fibroblast cellular density at the earlier time point potentially hasten the degradation of Laponite-containing PEG-D4 network.[62] Therefore, relatively

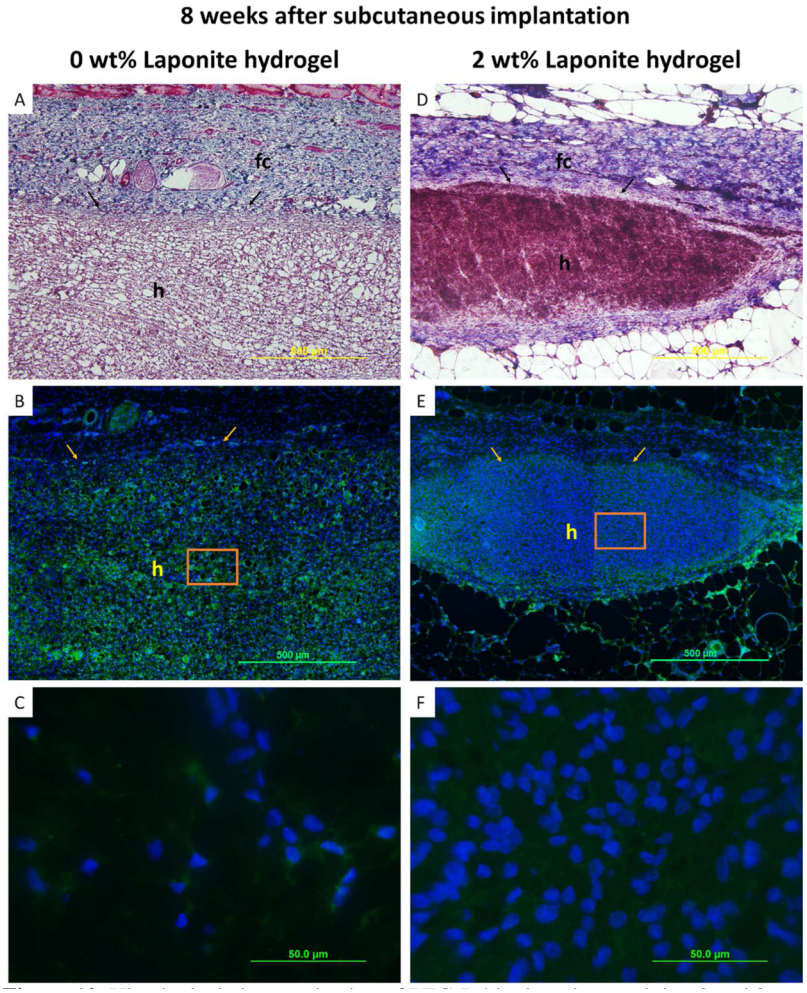

Figure 10. Histological characterization of PEG-D4 hydrogels containing 0 and 2 wt % Laponite and surrounding tissues after eight weeks of subcutaneous implantation. Masson's trichrome staining images for evaluating the overall tissue section morphology and the thickness of the fibrous capsule (fc) (A, D). Immunohistochemical staining images for evaluating the infiltration cell type and density (B, C, E, F). Cell nuclei were stained by DAPI (blue), fibroblasts were stained by marker S100A4 (green). (C) and (F) are the enlarged view of the orange boxes in (B) and (E), respectively. "h": hydrogel; arrows: interface between hydrogel and tissue.

thinner fibrous capsules are attributed to the host resolving the foreign-body response for the smaller Laponite-containing samples. No macrophages were observed for both hydrogel types (images not shown), and the samples were completely infiltrated with fibroblast, which appeared to be evenly distributed within the whole gel. Additionally, there was a significantly higher cell density in hydrogels containing 2 wt % Laponite as compared to that of Laponite-free sample.

Subcutaneous implantation results indicated that PEG-D4 nanocomposite is biocompatible. The thickness of fibrous capsule surrounding 2 wt % Laponite hydrogels at eight weeks postimplantation was significantly lower when compared to Laponite-free samples. This indicated that there is a reduced foreign-body reaction to the implanted nanocomposite.[44,63] Additionally, there was no macrophage present after eight weeks for samples containing either 0 or 2 wt % Laponite, indicating that these hydrogels did not induce prolonged inflammatory response. Other catechol-modified polymeric adhesives have also been demonstrated to elicit minimal inflammatory responses in vivo.[19,57] Additionally, Laponite has been previously shown to be biocompatible when incorporated into a hydrogel[33,34,64] with biocompatible degradation products (Na^+, $Si(OH)_4$, Mg^{2+}, Li^+).[30]

Most interestingly, Laponite-incorporated hydrogels displayed an enhanced level of cellular infiltration at both time points. Laponite has been previously reported to provide binding sites for cell attachment and proliferation.[33,34,64] The relatively small pore size (mesh size on the order of 70 Å)[40,65] in the PEG-D4 network provides physical hindrance for cellular ingrowth. However, the presence of dopamine-Laponite physical cross-links can potentially be broken and displaced by migrating cells. Cellular infiltration into synthetic, physically cross-linked networks have been previously demonstrated.[66] To induce cellular infiltration into inert and synthetic hydrogels, hydrogels are typically modified with cell-binding peptides (e.g., RGD) or other bioactive protein[67−69] or are designed to be susceptible to matrix metalloproteinase-mediated degradation,[57,70] which requires complicated and multistep chemical synthesis. Compared to these strategies, introducing Laponite into a hydrogel network offered a facile method to simultaneously promote bioactivity and adhesive property of a PEG-based adhesive. The formation of fibrous capsules surrounding PEG-D4 nanocomposite may hinder the molecular exchange between implanted materials and surrounding tissues, indicating that the adhesive may not be appropriate for repairing tissues that are rich in vasculatures.[71] However,

Laponite has previously been demonstrated to promote osteoblast proliferation, differentiation, and mineralization.[33] Additionally, Laponite shares much composition similarity to silica that has been previously suggested to serve as a cross-linking agent in connective tissue.[72] Nanocomposite adhesive described here may be a promising biomaterial for bone and connective tissue repair. Additional study is required to evaluate the effect of Laponite incorporation on the performance of adhesive in vivo.

CONCLUSION

We described an injectable nanocomposite tissue adhesive hydrogel based on dopamine-functionalized four-arm PEG and a synthetic nanosilicate, Laponite. Introduction of Laponite significantly increased the curing rate, bulk mechanical property, and adhesive property of the adhesive due to strong interfacial binding between dopamine and Laponite. The addition of Laponite did not alter the degradation rate and biocompatibility of PEG-D4. From subcutaneous implantation in rats, PEG-D4 nanocomposite hydrogels elicited minimal inflammatory response. Additionally, samples containing Laponite exhibited a significantly higher level of cell infiltration than that of the Laponite-free control, indicating that the addition of Laponite is potentially a simple and effective method to simultaneously promote bioactivity and adhesive performance of a bioinert, synthetic PEG-based adhesive.

ASSOCIATED CONTENT

Supporting Information

Schematic of nanocomposite hydrogel injectability, FTIR spectra of degraded hydrogel, and CD68 cell marker staining results. This material is available free of charge via the Internet at http://pubs.acs.org.

AUTHOR INFORMATION

Corresponding Author

*E-mail: bplee@mtu.edu. Phone: (906) 487-3262.

Author Contributions

§These authors contributed equally to this work

Notes

The authors declare no competing financial interest.

ACKNOWLEDGMENTS

This project was supported by National Institutes of Health (Grant No. GM104846) and Research Excellence Fund—Research Seed Grant provided by Michigan Technological University (MTU). R.S. was supported in part by MTU Michigan College/University Partnership Transfer Transition Program Partnered with the Michigan Louis Stokes Alliance for Minority Participation. The authors thank Dr. J. Goldman for his assistance with animal surgery.

REFERENCES

(1) Ikada, Y. In *Wound Closure Biomaterials and Devices;* Chu, C. C., von Fraunhofer, J. A., Greisler, H. P., Eds.; CRC Press, Inc.: Boca Raton, FL, 1997; Tissue Adhesives, pp 317−346.

(2) Mehdizadeh, M.; Yang, J. Design Strategies and Applications of Tissue Bioadhesives. *Macromol. Biosci.* **2013**, *13*, 271−288.

(3) Spotnitz, W. D. History of Tissue Adhesive. In *Surgical Adhesives and Sealants: Current Technology and Applications;* Sierra, D. H., Saltz, R., Eds.; Technomic Publishing Co., Inc.: Lancaster, PA, 1996; pp 3−11.

(4) Eriksen, J. R.; Bech, J. I.; Linnemann, D.; Rosenberg, J. Laparoscopic Intraperitoneal Mesh Fixation with Fibrin Sealant (Tisseel) Vs. Titanium Tacks: A Randomised Controlled Experimental Study in Pigs. *Hernia* **2008**, *12*, 483−491.

(5) Olivier ten Hallers, E. J.; Jansen, J. A.; Marres, H. A. M.; Rakhorst, G.; Verkerke, G. J. Histological Assessment of Titanium and Polypropylene Fiber Mesh Implantation with and without Fibrin Tissue Glue. *J. Biomed. Mater. Res., Part A* **2006**, *80A*, 372−380.

(6) Saltz, R.; Sierra, D.; Feldman, D.; Saltz, M. B.; Dimick, A.; Vasconez, L. O. Experimental and Clinical Applications of Fibrin Glue. *Plast. Reconstr. Surg.* **1991**, *88*, 1005−15 discussion 1016−7.

(7) Refojo, M. F.; Dohlman, C. H.; Koliopoulos, J. Adhesives in Ophthalmology: A Review. *Surv. Ophthalmol.* **1971**, *15*, 217−36.

(8) Fortelny, R. H.; Petter-Puchner, A. H.; Walder, N.; Mittermayr, R.; Öhlinger, W.; Heinze, A.; Redl, H. Cyanoacrylate Tissue Sealant Impairs Tissue Integration of Macroporous Mesh in Experimental Hernia Repair. *Surg. Endosc.* **2007**, *21*, 1781−1785.

(9) Blackburn, S. L.; Smyth, M. D. Hydrogel-Induced Cervicomedullary Compression after Posterior Fossa Decompression for Chiari Malformation - Case Report. *J. Neurosurg.* **2007**, *106*, 302−304.

(10) Mulder, M.; Crosier, J.; Dunn, R. Cauda Equina Compression by Hydrogel Dural Sealant after a Laminotomy and Discectomy Case Report. *Spine* **2009**, *34*, E144−E148.

(11) West, J. L.; Hubbell, J. A. Separation of the Arterial Wall from Blood Contact Using Hydrogel Barriers Reduces Intimal Thickening after Balloon Injury in the Rat: The Roles of Medial and Luminal Factors in Arterial Healing. *Proc. Natl. Acad. Sci. U.S.A.* **1996**, *93*, 13188−13193.

(12) Waite, J. H. Nature's Underwater Adhesive Specialist. *Int. J. Adhes. Adhes.* **1987**, *7*, 9−14.

(13) Waite, J. H. Adhesion a La Moule. *Integr. Comp. Biol.* **2002**, *42*, 1172−1180.

(14) Lee, B. P.; Messersmith, P. B.; Israelachvili, J. N.; Waite, J. H. Mussel-Inspired Adhesives and Coatings. *Annu. Rev. Mater. Res.* **2011**, *41*, 99−132.

(15) Lee, H.; Scherer, N. F.; Messersmith, P. B. Single Molecule Mechanics of Mussel Adhesion. *Proc. Natl. Acad. Sci. U.S.A.* **2006**, *103*, 12999−13003.

(16) Rzepecki, L. M.; Hansen, K. M.; Waite, J. H.Bioadhesives: Dopa and Phenolic Proteins as Component of Organic Composite Materials. In *Principles of Cell Adhesion;* Richardson, P. D., Steiner, M., Eds.; CRC Press, Inc.: Boca Raton, FL, 1995; pp 107−142.

(17) Sugumaran, M. Unified Mechanism for Sclerotization of Insect Cuticles. *Adv. Insect Physiol.* **1998**, *27*, 230−334.

(18) Guvendiren, M.; Brass, D. A.; Messersmith, P. B.; Shull, K. R. Adhesion of Dopa-Functionalized Model Membranes to Hard and Soft Surfaces. *J. Adhes.* **2009**, *86*, 631−645.

(19) Mehdizadeh, M.; Weng, H.; Gyawali, D.; Tang, L.; Yang, J. Injectable Citrate-Based Mussel-Inspired Tissue Bioadhesives with High Wet Strength for Sutureless Wound Closure. *Biomaterials* **2012**, *33*, 7972−83.

(20) Bilic, G.; Brubaker, C.; Messersmith, P. B.; Mallik, A. S.; Quinn, T. M.; Haller, C.; Done, E.; Gucciardo, L.; Zeisberger, S. M.; Zimmermann, R.; Deprest, J.; Zisch, A. H. Injectable Candidate Sealants for Fetal Membrane Repair: Bonding and Toxicity in Vitro. *Am. J. Obstet. Gynecol.* **2010**, *202*, 85.e1−9.

(21) Haller, C. M.; Buerzle, W.; Kivelio, A.; Perrini, M.; Brubaker, C. E.; Gubeli, R. J.; Mallik, A. S.; Weber, W.; Messersmith, P. B.; Mazza, E.; Ochsenbein-Koelble, N.; Zimmermann, R.; Ehrbar, M. Mussel-Mimetic Tissue Adhesive for Fetal Membrane Repair: An ex Vivo Evaluation. *Acta Biomaterialia* **2012**, *8*, 4365−70.

(22) Brodie, M.; Vollenweider, L.; Murphy, J. L.; Xu, F.; Lyman, A.; Lew, W. D.; Lee, B. P. Biomechanical Properties of Achilles Tendon Repair Augmented with Bioadhesive-Coated Scaffold. *Biomed. Mater. (Bristol, U. K.)* **2011**, *6*, 015014.

(23) Brubaker, C. E.; Kissler, H.; Wang, L.-J.; Kaufman, D. B.; Messersmith, P. B. Biological Performance of Mussel-Inspired Adhesive in Extrahepatic Islet Transplantation. *Biomaterials* **2010**, *31*, 420−427.

(24) Hong, S.; Yang, K.; Kang, B.; Lee, C.; Song, I. T.; Byun, E.; Park, K. I.; Cho, S.-W.; Lee, H. Hyaluronic Acid Catechol: A Biopolymer Exhibiting a Ph-Dependent Adhesive or Cohesive Property for Human Neural Stem Cell Engineering. *Adv. Funct. Mater.* **2013**, *23*, 1774−1780.
(25) Kastrup, C. J.; Nahrendorf, M.; Figueiredo, J. L.; Lee, H.; Kambhampati, S.; Lee, T.; Cho, S.-W.; Gorbatov, R.; Iwamoto, Y.; Dang, T. T. Painting Blood Vessels and Atherosclerotic Plaques with an Adhesive Drug Depot. *Proc. Natl. Acad. Sci. U.S.A.* **2012**, *109*, 21444−21449.
(26) Hoppe, A.; Güldal, N. S.; Boccaccini, A. R. A Review of the Biological Response to Ionic Dissolution Products from Bioactive Glasses and Glass-Ceramics. *Biomaterials* **2011**, *32*, 2757−2774.
(27) Hench, L. L. Genetic Design of Bioactive Glass. *J. Eur. Ceram. Soc.* **2009**, *29*, 1257−1265.
(28) Hench, L. L.; Paschall, H. A. Direct Chemical Bond of Bioactive Glass-Ceramic Materials to Bone and Muscle. *J. Biomed. Mater. Res.* **1973**, *7*, 25−42.
(29) Thompson, D. W.; Butterworth, J. T. The Nature of Laponite and Its Aqueous Dispersions. *J. Colloid Interface Sci.* **1992**, *151*, 236−243.
(30) Carlisle, E. M. Silicon: A Possible Factor in Bone Calcification. *Science* **1970**, *167*, 279−280.
(31) Reffitt, D. M.; Ogston, N.; Jugdaohsingh, R.; Cheung, H. F. J.; Evans, B. A. J.; Thompson, R. P. H.; Powell, J. J.; Hampson, G. N. Orthosilicic Acid Stimulates Collagen Type 1 Synthesis and Osteoblastic Differentiation in Human Osteoblast-Like Cells in Vitro. *Bone* **2003**, *32*, 127−135.
(32) Zreiqat, H.; Howlett, C. R.; Zannettino, A.; Evans, P.; Schulze-Tanzil, G.; Knabe, C.; Shakibaei, M. Mechanisms of Magnesium-Stimulated Adhesion of Osteoblastic Cells to Commonly Used Orthopaedic Implants. *J. Biomed. Mater. Res.* **2002**, *62*, 175−184.
(33) Gaharwar, A. K.; Schexnailder, P. J.; Kline, B. P.; Schmidt, G. Assessment of Using Laponite® Cross-Linked Poly(Ethylene Oxide) for Controlled Cell Adhesion and Mineralization. *Acta Biomater.* **2011**, *7*, 568−577.
(34) Gaharwar, A. K.; Rivera, C. P.; Wu, C. J.; Schmidt, G. Transparent, Elastomeric and Tough Hydrogels from Poly(Ethylene Glycol) and Silicate Nanoparticles. *Acta Biomater.* **2011**, *7*, 4139−48.
(35) Skelton, S.; Bostwick, M.; O'Connor, K.; Konst, S.; Casey, S.; Lee, B. P. Biomimetic Adhesive Containing Nanocomposite Hydrogel with Enhanced Materials Properties. *Soft Matter* **2013**, *9*, 3825−3833.
(36) Dalsin, J. L.; Lee, B. P.; Vollenweider, L.; Silvary, S.; Murphy, J. L.; Xu, F.; Spitz, A.; Lyman, A. Multi-Armed Catechol Compound Blends. U.S. Patent No. 8,119,742 (21 February 2012).
(37) Lee, B. P.; Dalsin, J. L.; Messersmith, P. B. Synthesis and Gelation of Dopa-Modified Poly(ethylene glycol) Hydrogels. *Biomacromolecules* **2002**, *3*, 1038−47.
(38) ASTM F2255−05 (2010), "Standard Test Method for Strength Properties of Tissue Adhesives in Lap-Shear by Tension Loading," ASTM International, West Conshohocken, PA, 2010, DOI: 10.1520/F2255-05R10, www.astm.org (accessed June 2013).
(39) Liu, Y.; Zhan, H.; Skelton, S.; Lee, B. P. Marine Adhesive Containing Nanocomposite Hydrogel with Enhanced Materials and Bioadhesive Properties. *MRS Online Proc. Libr.* **2013**, *1569*, mrss13−1569−LL05−09.
(40) Cencer, M. M.; Liu, Y.; Winter, A.; Murley, M.; Meng, H.; Lee, B. P. Effect of Ph on the Rate of Curing and Bioadhesive Properties of Dopamine Functionalized Poly(Ethylene Glycol) Hydrogels. *Biomacromolecules* **2014**, *15*, 2861−2869.
(41) ISO 10993−5: Biological Evaluation of Medical Devices. In *Part 5: Tests for Cytotoxicity: in Vitro Methods;* International Organization for Standardization: 2012.
(42) Huebsch, N.; Gilbert, M.; Healy, K. E. Analysis of Sterilization Protocols for Peptide-Modified Hydrogels. *J. Biomed. Mater. Res., Part B* **2005**, *74B*, 440−447.
(43) Kerby, R. E.; Tiba, A.; Culbertson, B. M.; Schricker, S.; Knobloch, L. Evaluation of Tertiary Amine Co-Initiators Using Differential Scanning Photocalorimetry. *J. Macromol. Sci., Part A: Pure Appl.Chem.* **1999**, *A36*, 1227−1239.
(44) Rujitanaroj, P. O.; Jao, B.; Yang, J.; Wang, F.; Anderson, J. M.; Wang, J.; Chew, S. Y. Controlling Fibrous Capsule Formation through Long-Term Down-Regulation of Collagen Type I (Col1a1) Expression by Nanofiber-Mediated Sirna Gene Silencing. *Acta Biomater.* **2013**, *9*, 4513−4524.
(45) Knop, K.; Hoogenboom, R.; Fischer, D.; Schubert, U. S. Poly(ethylene glycol) in Drug Delivery: Pros and Cons as Well as Potential Alternatives. *Angew. Chem., Int. Ed.* **2010**, *49*, 6288−6308.
(46) Yu, M.; Hwang, J.; Deming, T. J. Role of L-3,4-Dihydroxyphenylanine in Mussel Adhesive Proteins. *J. Am. Chem. Soc.* **1999**, *121*, 5825−5826.
(47) Sugumaran, M.; Semensi, V.; Kalyanaraman, B.; Bruce, J. M.; Land, E. J. Evidence for the Formation of a Quinone Methide During the Oxidation of the Insect Cuticular Sclerotizing Precursor 1,2-Dehydro-N- Acetyldopamine. *J. Biol. Chem.* **1992**, *267*, 10355−61.
(48) Kolhe, P.; Kannan, R. M. Improvement in Ductility of Chitosan through Blending and Copolymerization with Peg: Ftir Investigation of Molecular Interactions. *Biomacromolecules* **2003**, *4*, 173−180.
(49) Li, P.; Kim, N. H.; Hui, D.; Rhee, K. Y.; Lee, J. H. Improved Mechanical and Swelling Behavior of the Composite Hydrogels Prepared by Ionic Monomer and Acid-Activated Laponite. *Appl. Clay Sci.* **2009**, *46*, 414−417.
(50) Anseth, K. S.; Bowman, C. N.; Brannon-Peppas, L. Mechanical Properties of Hydrogels and Their Experimental Determination. *Biomaterials* **1996**, *17*, 1647−57.
(51) Peppas, N. A.; Bures, P.; Leobandung, W.; Ichikawa, H. Hydrogels in Pharmaceutical Formulations. *Eur. J. Pharm. Biopharm.* **2000**, *50*, 27−46.
(52) Yang, J.; Han, C.-R.; Zhang, X.-M.; Xu, F.; Sun, R.-C. Cellulose Nanocrystals Mechanical Reinforcement in Composite Hydrogels with Multiple Cross-Links: Correlations between Dissipation Properties and Deformation Mechanisms. *Macromolecules (Washington, DC, U. S.)* **2014**, *47*, 4077−4086.
(53) Narita, T.; Mayumi, K.; Ducouret, G.; Hébraud, P. Viscoelastic Properties of Poly (Vinyl Alcohol) Hydrogels Having Permanent and Transient Cross-Links Studied by Microrheology, Classical Rheometry, and Dynamic Light Scattering. *Macromolecules (Washington, DC, U. S.)* **2013**, *46*, 4174−4183.
(54) Rose, S. v.; Marcellan, A.; Hourdet, D.; Creton, C.; Narita, T. Dynamics of Hybrid Polyacrylamide Hydrogels Containing Silica Nanoparticles Studied by Dynamic Light Scattering. *Macromolecules (Washington, DC, U. S.)* **2013**, *46*, 4567−4574.
(55) da Silva, L. F. M.; Rodrigues, T. N. S. S.; Figueiredo, M. A. V.; de Moura, M. F. S. F.; Chousal, J. A. G. Effect of Adhesive Type and Thickness on the Lap Shear Strength. *J. Adhes.* **2006**, *82*, 1091−1115.
(56) Murphy, J. L.; Vollenweider, L.; Xu, F.; Lee, B. P. Adhesive Performance of Biomimetic Adhesive-Coated Biologic Scaffolds. *Biomacromolecules* **2010**, *11*, 2976−84.
(57) Brubaker, C. E.; Messersmith, P. B. Enzymatically Degradable Mussel-Inspired Adhesive Hydrogel. *Biomacromolecules* **2011**, *12*, 4326−34.
(58) Burke, S. A.; Ritter-Jones, M.; Lee, B. P.; Messersmith, P. B. Thermal Gelation and Tissue Adhesion of Biomimetic Hydrogels. *Biomed. Mater. (Bristol, U. K.)* **2007**, *2*, 203−210.
(59) Gaharwar, A. K.; Dammu, S. A.; Canter, J. M.; Wu, C. J.; Schmidt, G. Highly Extensible, Tough, and Elastomeric Nanocomposite Hydrogels from Poly(Ethylene Glycol) and Hydroxyapatite Nanoparticles. *Biomacromolecules* **2011**, *12*, 1641−50.
(60) Cao, H.; McHugh, K.; Chew, S. Y.; Anderson, J. M. The Topographical Effect of Electrospun Nanofibrous Scaffolds on the in Vivo and in Vitro Foreign Body Reaction. *J. Biomed. Mater. Res., Part A* **2010**, *93A*, 1151−1159.
(61) Ferreira, L.; Rafael, A.; Lamghari, M.; Barbosa, M. A.; Gil, M. H.; Cabrita, A. M. S.; Dordick, J. S. Biocompatibility of Chemoenzymatically Derived Dextran-Acrylate Hydrogels. *J. Biomed. Mater. Res., Part A* **2004**, *68A*, 584−596.

(62) Pan, H.; Jiang, H.; Chen, W. The Biodegradability of Electrospun Dextran/Plga Scaffold in a Fibroblast/Macrophage Co-Culture. *Biomaterials* **2008**, *29*, 1583−1592.
(63) Azab, A. K.; Doviner, V.; Orkin, B.; Kleinstem, J.; Srebnik, M.; Nissan, A.; Rubinstein, A. Biocompatibility Evaluation of Crosslinked Chitosan Hydrogels after Subcutaneous and Intraperitoneal Implantation in the Rat. *J. Biomed. Mater. Res., Part A* **2007**, *83A*, 414−422.
(64) Schexnailder, P. J.; Gaharwar, A. K.; Bartlett, R. L.; Seal, B. L.; Schmidt, G. Tuning Cell Adhesion by Incorporation of Charged Silicate Nanoparticles as Cross-Linkers to Polyethylene Oxide. *Macromol. Biosci.* **2010**, *10*, 1416−1423.
(65) Cruise, G. M.; Scharp, D. S.; Hubbell, J. A. Characterization of Permeability and Network Structure of Interfacially Photopolymerized Poly(Ethylene Glycol) Diacrylate Hydrogels. *Biomacromolecules* **1998**, *19*, 1287−1294.
(66) Zhang, J.; Tokatlian, T.; Zhong, J.; Ng, Q. K. T.; Patterson, M.; Lowry, W. E.; Carmichael, S. T.; Segura, T. Physically Associated Synthetic Hydrogels with Long-Term Covalent Stabilization for Cell Culture and Stem Cell Transplantation. *Adv. Mater.* **2011**, *23*, 5098−5103.
(67) Slaughter, B. V.; Khurshid, S. S.; Fisher, O. Z.; Khademhosseini, A.; Peppas, N. A. Hydrogels in Regenerative Medicine. *Adv. Mater.* **2009**, *21*, 3307−29.
(68) Seal, B. L.; Otero, T. C.; Panitch, A. Polymeric Biomaterials for Tissue and Organ Regeneration. *Mater. Sci. Eng., R* **2001**, *34*, 147−230.
(69) Seliktar, D. Designing Cell-Compatible Hydrogels for Biomedical Applications. *Science* **2012**, *336*, 1124−8.
(70) Lutolf, M. P.; Lauer-Fields, J. L.; Schmoekel, H. G.; Metters, A. T.; Weber, F. E.; Fields, G. B.; Hubbell, J. A. Synthetic Matrix Metalloproteinase-Sensitive Hydrogels for the Conduction of Tissue Regeneration: Engineering Cell-Invasion Characteristics. *Proc. Natl. Acad. Sci. U.S.A.* **2003**, *100*, 5413−5418.
(71) Ravin, A. G.; Olbrich, K. C.; Levin, L. S.; Usala, A. L.; Klitzman, B. Long- and Short-Term Effects of Biological Hydrogels on Capsule Microvascular Density around Implants in Rats. *J. Biomed. Mater. Res.* **2001**, *58*, 313−318.
(72) Schwarz, K. A Bound Form of Silicon in Glycosaminoglycans and Polyuronides. *Proc. Natl. Acad. Sci. U.S.A.* **1973**, *70*, 1608−12.